

Resonance structure of the cross section for photoionization of a hydrogen atom in an electric field

V. D. Kondratovich and V. N. Ostrovskii

Leningrad State University

(Submitted 16 March 1982)

Zh. Eksp. Teor. Fiz. **83**, 1256–1267 (October 1982)

The cross section for photoionization of a hydrogen atom in a uniform electric field is calculated with the use of a quasiclassical approximation that takes account of the above-barrier reflection, or the tunneling, that occurs during the motion of the electron in the final state. The structure in the energy dependence of the cross section is determined by the complex poles of the cross section. The motion of the poles that occurs as the parameters of the problem are varied is investigated. Equations for the positions and widths of the resonances in the regions below and above the effective potential barrier are derived and analyzed; the boundaries of these regions are defined. It is shown that the cross section in the vicinity of an isolated resonance forms a Fano profile, and approximate expressions are obtained for the profile index. A comparison with the results of numerical calculations is carried out, and recent experiments on the photoionization of rubidium atoms are discussed.

PACS numbers: 32.80.Fb

§1. INTRODUCTION

The development of methods of laser spectroscopy has made the detailed experimental investigation of highly excited atomic states in electric and magnetic fields possible (see Refs. 1–3 and the literature cited therein). Of special interest here are the hydrogenlike excited states of the atoms of the alkali metals, in view of the possible simplicity of their description. At excitation energies lower than the classical threshold for ionization of the atom in the electric field,¹ i.e., for $E \lesssim E_c$, the excited states form the wellknown Stark structure,^{4,5} but for the states with $E \gtrsim E_c$ the effect of the electric field is not weak, and cannot be treated as a perturbation.⁶ The analytical theory that takes account of this characteristic of the spectrum has not been sufficiently developed even for the hydrogen atom.

The study of the Stark effect is an integral part of the theoretical investigation of the cross section for photoionization of the hydrogen atom. The procedures developed by Damburg and Kolosov⁶ for the numerical computation of the positions and widths of the resonances, and based on the Lorentz parametrization of the resonance peaks, are well known. But Luc-Koenig and Bachelier⁷ have observed in a numerical calculation in which normalized wave functions were used that there are resonance peaks which differ in shape from the Lorentz peak.

The low clarity of the results and the ambiguity of many qualitative estimates obtained by means of numerical calculations indicate the need for an analytical theory. The natural means of constructing such a theory for strong fields is the quasiclassical approximation.

There have been established^{8–10} in the quasiclassical approximation simple equations for the positions of the resonances lying below the top of the potential barrier, and explicit expressions have also been found for the widths of these resonances. The results assume a compact form in the approximation most consistently used by Drukarev⁹ (see also Ref. 8), and consisting in the explicit separation of the contri-

butions of the centrifugal terms from the phase integrals and the subsequent expression of these integrals in terms of hypergeometric functions. This approximation is used in the present paper.

The above-barrier resonances, which also manifest themselves in experiments^{1,3} and numerical calculations,^{6,7} have thus far not been analytically investigated.

In the present paper we develop for the purpose of describing the resonance structure of the cross section a quasiclassical theory of photoionization of the hydrogen atom in a uniform electric field. In contrast to our previous paper,¹¹ here we take into consideration (using the separation of the variables in parabolic coordinates) the above-barrier-reflection and tunneling effects. This allows us to obtain for the cross section in the region $E < 0$ an expression that goes over continuously into the formulas obtained earlier¹¹ for $E > 0$ (§2). The investigation of the poles of the cross section in the complex plane of the separation z_1 (or $z_2 = Z - z_1$) (§3) enables us to identify unambiguously the resonances lying both below and above the barrier. The system of equations obtained for the below-barrier resonances goes over into Drukarev's result.⁹

As the energy is varied, the photoionization cross section poles trace out certain trajectories, the investigation of which (§4) is of fundamental interest. We also explain in §4 the experimentally observed^{1,2} general character of the dependence of the structure of the photoionization cross section on the polarization of the radiation.

The investigation of the shape of the resonance cross-section peaks (§5) shows that these peaks have the Fano profile¹² even in the case of the hydrogen atom. The assertion has been made before^{3,6,8,10} without sufficient justification that Lorentz resonance profiles are characteristic of the hydrogen atom. Approximate analytical expressions, applicable in a broad range of variation of the parameters of the problem, are obtained for the Fano parameters: the profile index q and the width Γ .

The expression for the resonance width generalizes the

previously obtained formulas,^{6,8,9} agreeing with them in the region of their applicability. As far as we know, this is the first time that expressions have been derived for the profile index and the energies and widths of the above-barrier resonances. In §6 the results obtained are compared with numerical calculations and experiment.

The paper was earlier presented in part at All-Union conferences.¹³

§2. PHOTOIONIZATION CROSS SECTION

As a result of the separation of the variables for the superposed Coulomb and homogeneous fields in parabolic coordinates $\xi = r + z, \eta = r - z, \varphi = \text{arctg}(y/x)$, the photoionization cross section in the dipole approximation can be represented in the form of a sum of partial cross sections¹¹:

$$\sigma_{|m|}(E) = \frac{(2\pi)^2}{c} \sum_m \sum_{n_\xi} \sigma_{n_\xi, m, E}, \quad (2.1)$$

$$\sigma_{n_\xi, m, E} = |\langle \Psi_0 | (\mathbf{r}, \mathbf{e}) | \Psi_{n_\xi, m, E} \rangle|^2, \quad (2.2)$$

where c is the velocity of light in vacuo, \mathbf{e} is the polarization vector of the light wave, and Ψ_0 is the initial-state wave function, the effect of the homogeneous field on which is neglected. The final-state wave function $\Psi_{n_\xi, m, E}$ is characterized by, besides the energy E , the discrete magnetic m and parabolic n_ξ quantum numbers. The states with fixed E and m values are degenerate in $n_\xi \geq 0$. The discreteness of n_ξ is due to the finiteness of the motion in the parabolic coordinate ξ . In the coordinate η , the motion is infinite, it being possible for the effective potential $V_z(\eta)$ to have the form of a barrier (see Figs. 1 and 2 in Ref. 11). Earlier¹¹ the quasiclassical approximation was applied by us to the above-barrier (i.e., $E > 0$) motion.

The main distinction of the present paper in respect of the computation of the partial cross sections $\sigma_{n_\xi, m, E}$ consists in the refinement of the quasiclassical description of the motion in the coordinate η by taking into account the above-barrier reflection (in the case of motion above the barrier) and the tunneling (in the case of motion below the barrier). For energies close to the top of the barrier, the latter can be approximated by a parabola, which allows us to introduce into the general quasiclassical expressions a correction that ensures the correct passage to the indicated limit (see Ref. 8, as well as the Appendix). The legitimacy of this approximation is confirmed by Harmin's recent investigation.¹⁰

We propose a new correction that guarantees the passage to the correct limit as $z_2/|k| \rightarrow 0$ [$k = (2E)^{1/2}$]; it is derived by comparing the corresponding asymptotic forms of the solution of the Coulomb problem with the quasiclassical wave function. Qualitatively, we can assert that this correction (see the Appendix) takes account of the potential-barrier asymmetry, whose role increases as $z_2/|k| \rightarrow 0$ (the dipole moment of the atom is oriented against the direction of the electric field). A similar correction should be introduced in the description of the motion in the ξ coordinate in the case when $E > 0$ (see the Appendix).

Let us give here the final expression for the partial cross sections, which it is convenient to treat as functions of the

separation constants z_1 and z_2 :

$$\sigma_{n_\xi, m, E} = 2^{3/2} \pi C^2 f(z_1) dz_1 / dS_+, \quad (2.3)$$

$$f(z_1) = \frac{(z_1 - z_2)^2}{(1 + e^{2s_-}) [1 + 2e^{2K} + 2e^K (1 + e^{2K})^{1/2} \cos 2\Phi]} \quad (m=0), \quad (2.4)$$

$$f(z_1) = \frac{z_1 z_2}{(1 + e^{2s_-}) [1 + 2e^{2K} + 2e^K (1 + e^{2K})^{1/2} \cos 2\Phi]} \quad (m=1). \quad (2.5)$$

The functions S_+ , S_- , Φ , and K are defined in the Appendix. The derivative in (2.3) is calculated at fixed E and \mathcal{E} . The expressions (2.4) and (2.5) are applicable for all energies when $z_2 < 0$ and for $E < 2(z_2 \mathcal{E})^{1/2}$ when $z_2 > 0$.

For $E \geq 2(z_2 \mathcal{E})^{1/2}$ the expressions obtained by us earlier,¹¹ and corresponding to the following formulas for $f(z_1)$:

$$f(z_1) = \frac{(z_1 - z_2)^2}{(1 + e^{-2\pi z_1/h})(1 + e^{-2\pi z_2/h})} \quad (m=0), \quad (2.6)$$

$$f(z_1) = \frac{z_1 z_2}{(1 - e^{-2\pi z_1/h})(1 - e^{-2\pi z_2/h})} \quad (m=1), \quad (2.7)$$

are valid.

For the hydrogenic wave function $\Psi_0 = \pi^{-1/2} \alpha^{3/2} \exp(-\alpha r)$ of the initial s state, the coefficient C in (2.3) has the form

$$C = \frac{16\alpha^{3/2} (\alpha - Z/2)}{\pi^{1/2} (\alpha^2 + 2E)^3} \begin{cases} \exp\left(-\frac{2Z}{k} \text{arctg} \frac{k}{\alpha}\right), & E > 0, \\ [(\alpha - |k|)/(\alpha + |k|)]^{Z/|k|}, & E < 0. \end{cases} \quad (2.8)$$

The integral $S_+(z_1, E)$ enters into the Bohr-Sommerfeld quantization rule for the finite motion in the coordinate ξ :

$$S_+(z_1, E) = \pi [n_\xi + 1/2 (|m| + 1)], \quad (2.9)$$

which gives the function $z_1(n_\xi, E, m)$. In (2.9), as in Ref. 11, we have used Drukarev's approximation,⁹ which consists in the explicit separation of the contribution of the centrifugal term to the phase integral.

§3. POLES OF THE PHOTOIONIZATION CROSS SECTION

To investigate and explain the singularities of the photoionization cross section, let us consider the cross section to be a function of the complex final energy E . In practice, it is convenient to consider the plane of the complex separation constant z_1 , which is related to the energy according to Eq. (2.9). Since the boundary conditions for the wave function in parabolic coordinates do not depend on z_1 , it can be expected that the exact partial cross sections will be analytic functions of z_1 . It follows from the formulas (2.3)–(2.7) that the singularities of the cross section are poles, which naturally divide into two series according to the two factors in the denominator of the function $f(z_1)$. In view of the symmetric disposition of the poles with respect to the real axis, below we consider only those poles that lie in the upper half-plane of z_1 (correspondingly, those in the lower half-plane of $z_2 = Z - z_1$).

The simplest case is the one in which the expression (2.6) or (2.7) for $f(z_1)$ is used for all physically important values of z_1 . This corresponds to the approximation adopted in our previous paper,¹¹ and, as will be seen below, it is correct when $E \geq \mathcal{E}^{2/3}$. Numbering the poles of the function $f(z_1)$

inside each series by integers $l, n_2 \geq 0$, we obtain for them the expressions

$$z_{1l}^{(1)} = ik[l + 1/2(|m| + 1)], \quad (3.1)$$

$$z_{1n_2}^{(2)} = ik[n_2 + 1/2(|m| + 1)] + Z. \quad (3.2)$$

For $f(z_1)$ given by the formulas (2.4) and (2.5), the poles of the series are respectively given by the equations

$$S_-(z_1, E) = i\pi[l + 1/2(|m| + 1)], \quad (3.3)$$

$$G(z_2, E) = 2\pi[n_2 + 1/2(|m| + 1)], \quad (3.4)$$

where

$$G(z_2, E) = 2\Phi_0 + 1/2 i \ln(1 + e^{-2K}) \quad (3.5)$$

and the functions Φ_0 and K are defined in the Appendix.

It is convenient to characterize the disposition of the poles by the parameters

$$z_c = E^2/4\mathcal{E} = (E/E_c)^2 Z, \quad \nu = |k|^3/\mathcal{E}. \quad (3.6)$$

For $\nu \lesssim l$, the positions of the poles of the first series do not depend on the energy, and are completely determined by the strength of the electric field:

$$z_{1l}^{(1)} \approx \frac{3^{1/2}\pi^2 e^{i\pi/4}}{[\Gamma(1/4)]^{3/2}} \mathcal{E}^{1/4} \left(l + \frac{|m| + 1}{2} \right)^{3/4}. \quad (3.7)$$

In the case $\nu \gtrsim l$ the positions of the poles are given by the relation (3.1) with k replaced by $|k|$, and do not depend on the field strength. The poles of the first series have practically no effect on the energy dependence of the cross section in the case when $E < 0$, since in this case the spectral $z_1(n_\xi)$ values obtained from (2.9) are considerably far from these poles.

For the second series of poles, when the energy is lower than the top of the potential barrier $V_2(\eta)$ [and $\exp(-2K) \lesssim 1$], the equation determining the poles assumes the form

$$\Phi_0(z_2, E) = \pi[n_2 + 1/2(|m| + 1)]. \quad (3.8)$$

It gives together with (2.9) the positions of the levels of the Stark multiplet and the corresponding values of the separation constants z_{2s} and z_{1s} , $z_{1s} + z_{2s} = Z$ (see Ref. 9, where this system of equations is reduced to a form suitable for computations, and Ref. 14, where examples of the calculation are given. Thus, n_2 has the meaning of a parabolic quantum number, determining together with $n_1 = n_\xi$ and m the state of the atom in the presence of an external electric field. The imaginary part of the pole $z_2(n_2)$ is connected with the width of this state, and is found, when $\exp(-2K) \lesssim 1$, from (3.4) and (3.5), where the imaginary term is treated as a small correction:

$$z_2 \approx z_{2s} - i \frac{\ln(1 + e^{-2K})}{2\partial\Phi/\partial z_2}. \quad (3.9)$$

As the energy is increased, the pole with a given value of n_2 moves away from the real axis, describing some trajectory in the process.

The poles with $\text{Re} z_2 > z_c$ correspond to resonances lying above the top of the barrier $V_2(\eta)$. The energy at which the position of the resonance corresponds to the top of the barrier $V_2(\eta)$ is called in the literature the "parabolic critical

energy," and is denoted by E_{pc} . It turns out to be possible to derive in the quasiclassical approximation analytic expressions for this energy as functions of n_1 and n_2 , i.e., expressions that determine the order in which the resonances rise above the top of the barrier.

The equation $\text{Re} z_2(n_2) = z_c$ together with (3.6) and (3.8) gives E_{pc} as a function of n_2 :

$$E_{pc}(n_2) = - \left[\frac{3\pi}{2} \left(n_2 + \frac{|m| + 1}{2} \right) \mathcal{E} \right]^{2/3}, \quad (3.10)$$

from which it can be seen that all the resonances for energies $E > E_{pc}(0) = - [3\pi(|m| + 1)\mathcal{E}]^{2/3}$ are above-barrier resonances. The inequality $E_{pc}(0) < 0$ contradicts the assertion made in Ref. 7 that values of $E_{pc} > 0$ exist. The condition $z_1(n_1) = Z - z_c$ together with (2.9) and (3.6) gives E_{pc} as a function of n_1 :

$$E_{pc}(n_1) = -2(Z\mathcal{E})^{1/2} (1 - \tau)(1 + \tau)^{-1}, \quad (3.11)$$

where $0 < \tau < 1$ is determined from the equation

$$\frac{2\tau}{(1 + \tau)^{3/2}} F(-1/2, 1/2, 2; -\tau) = \left(\frac{\mathcal{E}}{Z^3} \right)^{1/4} \left(n_1 + \frac{|m| + 1}{2} \right), \quad (3.12)$$

in which $F(a, b, c; z)$ is a hypergeometric function.

Equations (3.10)–(3.12) allow us to classify the resonances into above- and below-barrier resonances at any value of the electric field. Indeed, from (3.10)–(3.12) we can derive a universal relation between the quantities $X = \mathcal{E}^{1/4} Z^{-3/4} [n_2 + 1/2(|m| + 1)]$ and $Y = \mathcal{E}^{1/4} Z^{-3/4} [n_1 + 1/2(|m| + 1)]$:

$$\tau = \frac{1 - 2^{-3/2} (3\pi X)^{3/2}}{1 + 2^{-3/2} (3\pi X)^{3/2}}, \quad Y = \frac{2\tau}{(1 + \tau)^{3/2}} F(-1/2, 1/2, 2; -\tau). \quad (3.13)$$

Figure 1 shows a plot of the function $Y(X)$. The points located below this curve correspond to below-barrier states. We can, by finding the area under the curve through integration, obtain a simple expression for the total number of below-barrier states with fixed $m \ll \mathcal{E}^{-1/4} Z^{3/4}$; it is equal to

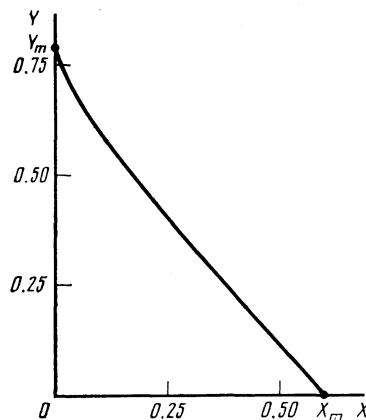


FIG. 1. The function $Y(X)$, (3.13), determining the division of the resonances into below- and above-barrier resonances ($X_m = 2^{5/2}/3\pi$, $Y_m = \Gamma^2(1/4)/3\pi^{3/2}$). The region under the curve corresponds to the below-barrier resonances $E < E_{pc}$.

$(2\pi)^{1/2} \Gamma^{-2}(\frac{1}{4}) Z^{3/2} \mathcal{E}^{-1/2}$. The point $(X_m, 0)$ on the graph determines the below-barrier resonance with the highest possible—for a given field intensity— n_2 quantum number (and $n_1 = 0$); the point $(0, Y_m)$, the highest below-barrier resonance with $n_2 = 0$ (and with the highest possible n_1 value for a below-barrier resonance). The $E_{pc}(n_1, m)$ values determined from Eqs. (3.11) and (3.12) are in good agreement with the values found in Ref. 7 by numerical computation in the region $E < 0$.

The system (3.13) allows us, when n_1, n_2 , and m are given, to determine the critical value \mathcal{E}_{pc} of the field intensity and [with the aid of (3.11)] the corresponding E_{pc} value. The scaling laws established for the Stark spectrum by Drukarev⁹ manifest themselves here: the reduced values of the critical field and critical energy $\mathcal{E}_{pc} n^4$ and $E_{pc} n^2$ (n is the principal quantum number) depend only on the ratios $n_1/n, n_2/n$, and $(|m| + 1)/n$:

$$\mathcal{E}_{pc} n^4 = \frac{2^{10} Z^3}{(3\pi v_2)^4} \left(\frac{1-\tau}{1+\tau} \right)^6, \quad E_{pc} n^2 = - \frac{2^8 Z^2}{(3\pi v_2)^2} \left(\frac{1-\tau}{1+\tau} \right)^4, \quad (3.14)$$

where $0 < \tau < 1$ is determined from the equation

$$\frac{3\pi}{2^{1/2}} \frac{\tau}{(1-\tau)^{1/2}} F(-1/2, 1/2, 2; -\tau) = \frac{v_1}{v_2}, \quad (3.15)$$

$$v_1 = n_1/n + 1/2 (|m| + 1)/n, \quad v_2 = n_2/n + 1/2 (|m| + 1)/n. \quad (3.16)$$

The same scaling laws manifest themselves¹⁵ when the contribution of the centrifugal terms is taken into account exactly in the evaluation of the phase integrals of the quasiclassical approximation and in the determination of the peak of the effective potential barrier, but this approach leads to more complicated expressions for E_{pc} and \mathcal{E}_{pc} .

§4. TRAJECTORIES DESCRIBED BY THE POLES UPON THE VARIATION OF THE ENERGY

We can, by separating out the dominant terms in Eq. (3.4) for $E \gtrsim E_{pc}$, obtain an equation describing the motion of a pole in the above-barrier region:

$$w^3 + 3\epsilon w + 2 = 0, \quad (4.1)$$

where $w = z_2/z_0, \epsilon = -E/E_0$,

$$z_0 = \frac{8\pi^{3/4}}{[\Gamma(1/4)]^{3/4}} z_{pc}, \quad E_0 = \frac{3\pi^{1/4}}{[\Gamma(1/4)]^{1/4}} E_{pc} \quad (4.2)$$

and we have used the notation $z_{pc} = E_{pc}^2/4\mathcal{E}$.

Let us qualitatively describe the motion in the complex z_1 plane of the poles determined by Eq. (3.4) as the energy increases [the disposition of the poles of the first series (3.3), which do not contribute to the structure of the cross section in the region $E < 0$, is described in §3]. Let us consider in the z_1 plane the circles C_0 and C_Z with radius z_c and centers at the points $z_1 = 0$ and $z_1 = Z$, i.e., $z_2 = 0$ (Fig. 2). Inside the circle C_Z the poles $z_1(n_2) = Z - z_2(n_2)$ are located near the real axis. The distance from the axis increases as we approach the boundary of the circle. A resonance appears in the cross section when the real part of the pole $z_1(n_2, E)$ coincides with some value of the spectrum $z_1(n_1, E)$ determined by Eq. (2.9) with $n_\xi = n_1$. As the energy increases, the points $z_1(n_1)$ move to the left along the real axis, while the poles inside the circle C_Z move to the right ($E < 0$) practically along the real axis. In the process, the radius of the circle C_Z decreases faster, so that the poles successively find themselves outside the circle, after which they move away from the real axis along the trajectories determined by Eq. (4.1) (see Fig. 2), approaching the straight line $\arg(z_1 - Z) = 2\pi/3$ as $E \rightarrow 0$.

The spectrum $z_1(n_1)$ differs little from the Coulomb spectrum when $z_1(n_1) \lesssim z_c$, i.e., inside the circle C_0 . Thus, the circles C_0 and C_Z contain those spectral values of $z_1(n_1)$ and $z_1(n_2)$ for which the homogeneous field has little effect on the motions in the coordinates ξ and η , respectively. Such a region exists for both coordinates at once only when $z_c > Z/2$, i.e., when $E \lesssim -(2Z\mathcal{E})^{1/2}$. For the resonances of this region, $z_1 \approx z_2$, i.e., the value of the additional integral of the motion $\beta = z_1 - z_2$ differs little from zero. Near the Coulomb center, β coincides with the component of the Runge-Lenz vector along the direction of the field,¹¹ so that, for the resonances under consideration, this vector is perpendicular to the direction of the field. Such states are populated largely by σ -polarized light ($e \perp \vec{\mathcal{E}}$). In the case of ionization by π -polar-

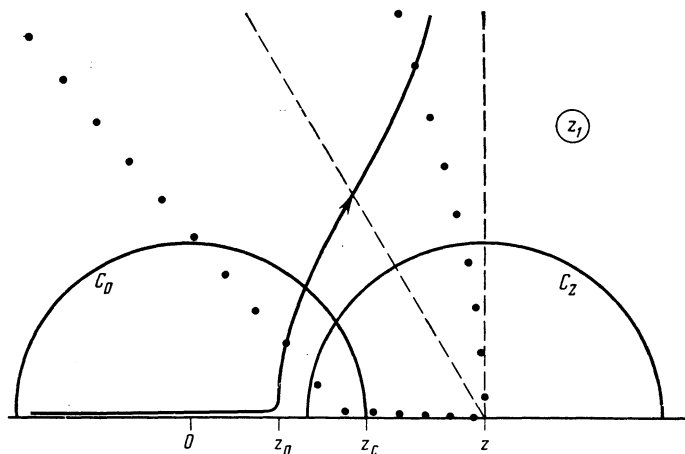


FIG. 2. Disposition of the series, determined by Eq. (3.4), of cross-section poles in the complex z_1 plane (only the upper half-plane is shown). The poles for $E < 0$ lie below, and those for $E > 0$ lie above, the straight line $\arg(z_1 - Z) = (2/3)\pi$. The pole closest to the point $z_1 = Z$ corresponds to $n_2 = 0$. The continuous line depicts the trajectory described by a pole as the energy increases.

ized light waves ($e\|\vec{\mathcal{E}}$), the states with $z_1 \approx 0$ and $z_1 \approx Z$ are populated, which gives rise to a significantly lower—in comparison with the preceding case—density of resonance peaks of appreciable height in the region $E > E_c$. As the energy increases ($E < 0$), the width of the resonances with $n_2 = 0$ [to which correspond, according to (3.8), z_1 values close to Z] increases most slowly, since the potential barrier $V_2(\eta)$ is highest in their case. As a result of this, the structure is preserved right up to energies $E \approx 0$ in ionization by π -polarized light, whereas the denser resonance structure in the case of σ polarization is concentrated in the lower-energy region $E \lesssim -(2Z\mathcal{E})^{1/2}$. Such dependence of the density of the resonance peaks on the light-wave polarization is observed in experiment.^{1,2}

As $E \rightarrow 0$, the circles C_0 and C_Z contract each to a point, which corresponds to the exertion of a strong influence by the electric field on the Coulomb center at $E \rightarrow 0$.

As the energy $E > 0$ increases further, the circles C_0 and C_Z again expand. The poles inside the circle C_Z lie on the diameter perpendicular to the real axis, and their positions do not depend on the electric-field strength [see the formulas (3.1) and (3.2) and Fig. 2]. The poles of the first series inside the circle C_0 lie on the imaginary axis. The poles closest to the real axis exert the strongest influence on the magnitude of the cross section, so that the formulas (2.6) and (2.7) can be used to describe the photoionization cross section in the region $E \gtrsim \mathcal{E}^{2/3}$. In this energy region, the positions of the poles with $l = 0$ and $n_2 = 0$ are given by the relations (3.1) and (3.2).

§5. RESONANCE FEATURES OF THE PHOTOIONIZATION CROSS SECTION

When the electron energy in the final state is lower than the classical ionization threshold E_c , the photoionization proceeds largely via the resonance Stark states. There occurs in the region $E > E_c$ a background corresponding to the possibility of above-barrier infinite photoelectron motion. Superposed on this background are peaks corresponding to below- and above-barrier resonances whose widths are smaller than the Stark splitting. We can show on the basis of the results presented below [see (5.4)] that the number of such above-barrier resonances with a given value of the quantum number n_2 is proportional to $[z_{pc}(n_2)]^{-1/2}$. Thus, in the case in which $n_2 = 0$ and the field intensity $\mathcal{E} = 4335$ V/cm (the field applied by Freeman *et al.* in their experiment¹) there can be as many as twenty of them. The energy dependence of the total cross section in the vicinity of such a resonance is determined by the partial cross section with the quantum number of the resonance. The resonance energy E_r is given by the system of equations (2.9) (with $n_s = n_1$) and (3.8) on condition that $z_1 + z_2 = Z$.

Near E_r , the magnitude of the partial cross section is determined by a pair of poles $z_2(n_2)$ and $z_2^*(n_2)$ of the function (2.4) or (2.5). Taking into account the fact that the energy dependence of $z_1(n_1)$ is given by Eq. (2.9), while the position of the pole $z_2(n_2)$ is given by Eq. (3.4), and also neglecting the small quantity $\exp(2S_-)$ in (2.4), we obtain a representation of the partial cross section near E_r in the form of a resonance

Fano profile:

$$\sigma_{n_1,0E} = \frac{\pi C^2}{2^{1/2}} |z_1 - z_2|^2 \left\{ \left[\left| \frac{\partial G}{\partial z_2} \right| (1+q^2) \operatorname{Im} S_+ \right]^{-1} \left(\frac{q^2 - 1}{1 + \varepsilon^2} + \frac{2q\varepsilon}{1 + \varepsilon^2} \right) + \frac{1}{2} \frac{\partial z_1}{\partial S_+} e^{-2\kappa} \right\}, \quad (5.1)$$

where

$$q = -\operatorname{ctg}(\alpha/2), \quad \varepsilon = (E - E_r) / (\Gamma/2), \quad (5.2)$$

$$\alpha = \arg(\partial G / \partial z_2) - 2 \arg(z_1 - z_2), \quad (5.3)$$

$$\Gamma = 2 \operatorname{Im} S_+ / \operatorname{Re} \left(\frac{\partial S_+}{\partial E} + \frac{\partial S_+}{\partial z_1} \frac{\partial G / \partial E}{\partial G / \partial z_2} \right); \quad (5.4)$$

all the quantities are computed at the location of the pole $z_1(n_2)$. The expression for the cross section $\sigma_{n_1,1E}$ is obtained, in accordance with (2.5), by replacing $|z_1 - z_2|^2$ by $|z_1 z_2|$ in (5.1) and $2 \arg(z_1 - z_2)$ by $\arg(z_1 z_2)$ in (5.3). The formula (5.4) is applicable in the case when the width Γ is smaller than the distance between resonances with quantum numbers differing by unity, a condition which corresponds to the inequality $\operatorname{Im} S_+ \lesssim 1$.

The possession by the resonances in a superposed Coulomb and homogeneous fields of Fano profiles corresponds to the interaction of the discrete Coulomb spectrum with the continuous spectrum for the motion in the homogeneous field. This interaction is strongest in the neighborhood of $E = 0$, the condensation point of the Coulomb spectrum. The characteristic scale for the energy region in which this interaction is appreciable is the magnitude E_c of the classical ionization threshold. The profile index q is determined by the resonance width and the density of states (the first term in (5.3), as well as the nonuniformity in the population of the quasibound state lying within the limits of the width of the resonance in the case of photoionization [the second term in (5.3)]. The last term in (5.1) gives the magnitude of the background part, due to tunneling through the potential barrier, of the cross section.

For the resonances whose widths are much smaller than the Stark splitting, the expressions (5.1)–(5.4) admit of further simplification. Let us given here only the formula for the resonance width in order to compare it with previously proposed approximations^{6,9}:

$$\Gamma = \frac{\partial S_+ / \partial z_1 \ln(1 + e^{-2\kappa})}{2 \partial (S_+, \Phi) / \partial (z_1, E)}, \quad (5.5)$$

where all the quantities are computed with z_1 and z_2 that are a solution to the system (2.9) and (3.8). For the below-barrier resonances (i.e., for $E \lesssim E_{pc}$) we have

$$\partial (S_+, \Phi) / \partial (z_1, E) \approx (\partial S_+ / \partial z_1) (\partial \Phi / \partial E),$$

(the error introduced by this substitution decreases with decreasing n_2). Setting also $\ln(1 + e^{-2\kappa}) \approx e^{-2\kappa}$, we arrive at the Drukarev approximation,⁹ which agrees with the Damburg-Kolosov approximation.⁶ The use of the correction (A.9) proposed by us for the barrier asymmetry significantly improves the agreement with the numerical calculation.⁶ We can simplify the expression (5.5) further in the various energy regions and for different relations between n_1 and n_2 , and

obtain a number of simple approximate formulas for the resonance widths.

The above-barrier resonances with large widths can be described with the use of the equation (4.1) of the pole trajectory; the above-barrier resonances in the energy region $E \gtrsim |E_{pc}|$, with the expression (3.2).

§6. COMPARISON WITH NUMERICAL COMPUTATIONS AND EXPERIMENT

The numerical-calculation data on the Stark spectrum^{6,7} correspond largely to the Lorentz parametrization of the resonance peaks. We can, by Lorentz parametrizing the peak of the Fano profile for the resonance energy E_F , the width Γ_F , and the profile index q , arrive at the following values for the resonance energy E_L and the width Γ_L :

$$E_L = E_F + \Gamma_F / 2q, \quad \Gamma_L = \Gamma_F (1 + q^{-2}). \quad (6.1)$$

It can be seen from these relations that, for a sufficiently small resonance width and a sufficiently large profile index $q \gg 1$, the difference in the peak-parametrization modes does not play a significant role. The parameters Γ and q have values that satisfy these requirements in the case of resonances lying sufficiently far below the top of the effective-potential barrier $V_2(\eta)$, i.e., in the energy region $E \lesssim E_{pc}$. In the opposite case the difference is appreciable.

Using the quasiclassical expressions obtained, we computed the parameters of nearly forty resonances for which numerical-calculation data were available.^{6,7} We determined the resonance energy from the system of equations (2.9) and (3.8), using in Eq. (3.8) the parabolic-barrier correction (A.7), which reduces by an order of magnitude the error made when the energies are determined in the quasiclassical approach. The energy values found are in good agreement with the numerical-calculation data in both the subbarrier region (with a relative deviation of about 10^{-5}) and the above-barrier (i.e., $E \gtrsim E_{pc}$) region, but the deviation from the numerical-calculation data increases with increasing energy. The recalculation of the resonance energy in accordance with (6.1) improves the coincidence significantly (by a considerable factor) in the case of the resonances located close to and above the top of the effective potential barrier (the numerical calculations reported in Refs. 6 and 7 are based on the Lorentz parametrization of the profiles). This suggests that the interpretation of the numerical calculations should be improved by allowing for the correct parametrization.

The expression (5.5) together with the correction (A.9) for the barrier asymmetry provides a good approximation to the resonance width in a broad range of electric-field intensities (below- and above-barrier resonances) and for any relation between the quantum numbers n_1 and n_2 (different orientations of the dipole moment of the atom). The relative error can be as high as 10^{-3} in the subbarrier region ($E \lesssim E_{pc}$), but is lower in the case of the above-barrier resonances (i.e., in the region $E \gtrsim E_{pc}$). But there are also discrepancies in the values obtained for the above-barrier resonance width in the two published numerical calculations.^{6,7} A detailed comparison for various versions of the approximate formulas will be published separately together with ex-

TABLE I. Parameters of some resonance peaks from the region $-36 \text{ cm}^{-1} < E < -30 \text{ cm}^{-1}$ of the photoionization spectrum of the hydrogen atom in a field of intensity $\mathcal{E} = 158 \text{ V/cm}$ ($m = 0$ in the final state).

n_1	n_2	$-E_F, \text{ cm}^{-1}$	$\Gamma, \text{ a.u.}$	$-q$
40	10	30.225	$2.33 \cdot 10^{-8}$	122
39	11	31.411	$1.03 \cdot 10^{-7}$	29.3
38	12	32.602	$3.28 \cdot 10^{-7}$	11.6
37	13	33.782	$1.93 \cdot 10^{-6}$	7.17
36	13	35.664	$1.27 \cdot 10^{-7}$	227

amples illustrating the parabolic-critical-energy calculation.

Fano resonance-peak profiles have been experimentally observed in the photoionization cross section for the rubidium atom.³ The values $\Gamma = 0.13 \text{ GHz} = 2.0 \times 10^{-8} \text{ a.u.}$ and $q = 3.3$ were obtained in an electric field of intensity $\mathcal{E} = 158 \text{ V/cm}$ for a resonance energy of $E_F = 33.614 \text{ cm}^{-1}$. We have computed for the hydrogen atom the spectral region containing the indicated energy value. In Table I we present the parameters of fairly narrow peaks with profile indices $q \gtrsim -10^3$ from this spectral region. Such peaks are least subject to distortion by the instrumental effects, and their parameters are easy to measure. The resonance with $n_1 = 37$ and $n_2 = 13$ is an above-barrier resonance, and the rest are below-barrier resonances. The photoionization spectrum of the hydrogen atom, like that of the rubidium atom, is characterized by a developed structure. But it differs from the spectrum of the rubidium atom in that its resonances are disposed differently, there is a different relationship between the magnitude of the profile index and the width, and the profile index is opposite in sign. The last circumstance is, apparently, a manifestation of the mixing of the Rydberg states as a result of the deviation of the field of the atomic core from the Coulomb field.

APPENDIX

Here we present the definitions of the quantities used in the quasiclassical approximation and the expression for the corrections. All the integrals can be expressed in terms of the hypergeometric function in both the below-barrier⁹ and the above-barrier case.

1. The barrier index $K(z_2, E, \mathcal{E})$ is defined by the relation

$$K = \text{Im} \int_{\eta_-}^{\eta_+} \tilde{p}_\eta d\eta, \quad (A.1)$$

where the η_\pm are the roots of the modified¹¹ momentum \tilde{p}_η of the motion in the coordinate $\eta (\text{Im} \eta_+ \gg \text{Im} \eta_-)$:

$$\tilde{p}_\eta = (E/2 + z_2/\eta + \mathcal{E}\eta/4)^{1/2}, \quad \eta_\pm = [-E \pm (E^2 - 4z_2\mathcal{E})^{1/2}] / \mathcal{E}. \quad (A.2)$$

The function K is positive in the below-barrier case and negative in the above-barrier region.

2. The phase integral $\Phi(z_2, E, \mathcal{E})$ for the motion in the coordinate η is defined as

$$\Phi = \Phi_0 - |m| \pi / 2, \quad \Phi_0 = \text{Re} \int_0^{\eta_+} \tilde{p}_\eta d\eta. \quad (A.3)$$

3. The phase integral for the motion in the coordinate ξ

is

$$S_+(z_1, E, \mathcal{E}) = \operatorname{Re} \int_0^{\xi_+} \tilde{p}_i d\xi, \quad (\text{A.4})$$

$$\tilde{p}_i = (E/2 + z_1/\xi - \mathcal{E}\xi/4)^{1/2},$$

$$\xi_{\pm} = [E \pm (E^2 + 4z_1\mathcal{E})^{1/2}] / \mathcal{E} \quad (\operatorname{Im} \xi_+ \geq \operatorname{Im} \xi_-). \quad (\text{A.5})$$

4. The function $S_-(z_1, E, \mathcal{E})$ is defined by the relation

$$S_- = \operatorname{Im} \int_0^{\xi_-} \tilde{p}_i d\xi + i|m|\pi/2. \quad (\text{A.6})$$

5. The correct description of the resonances near the top of the barrier is achieved⁸ through the introduction of a parabolic-barrier correction, i.e., through the replacement of Φ_0 by $\Phi_0 + \sigma$, where

$$\sigma = \frac{1}{2} [\arg \Gamma(1/2 + iK/\pi) - (K/\pi) \ln |K/\pi| + K/\pi]. \quad (\text{A.7})$$

6. Qualitatively, the meaning of the introduction of the correction for the potential-barrier asymmetry is given in §2. Quantitatively, this correction consists in the replacement of K by $K + \kappa$, where

$$\kappa = \ln \Gamma \left(\frac{|m|+1}{2} + \frac{z_2}{|k|} \right) - \left(\frac{|m|}{2} + \frac{z_2}{|k|} \right) \ln \frac{z_2}{|k|} + \frac{z_2}{|k|} - \frac{1}{2} \ln(2\pi). \quad (\text{A.8})$$

In the same approximation, $z_2/|k| \approx \Phi/\pi + |m|/2 = n_2 + (|m|+1)/2$; consequently,

$$\kappa = \ln[(n_2 + |m|)!] - \left(n_2 + |m| + \frac{1}{2} \right) \ln \left(n_2 + \frac{|m|+1}{2} \right) + n_2 + \frac{|m|+1}{2} - \frac{1}{2} \ln(2\pi). \quad (\text{A.9})$$

7. The correction for the asymmetry of the potential well $V_1(\xi)$ for $E > 0$ consists in the replacement of S_+ by $S_+ + \sigma_+$, where

$$\sigma_+ = -\frac{\pi}{4} |m| - \arg \Gamma \left(\frac{|m|+1}{2} + i \frac{z_1}{k} \right) + \frac{z_1}{k} \ln \left| \frac{z_1}{k} \right| - \frac{z_1}{k}. \quad (\text{A.10})$$

¹¹ $E_c = -2(Z\mathcal{E})^{1/2}$; here and below, unless otherwise stated, we use atomic units, Z is the charge of the atomic core (for the hydrogen atom $Z = 1$), and \mathcal{E} is the electric-field intensity; $E = 0$ corresponds to the photon energy, equal to the ionization potential of the atom.

¹R. R. Freeman, N. P. Economou, G. C. Bjorklund, and K. T. Lu, Phys. Rev. Lett. **41**, 1463 (1978); R. R. Freeman and N. P. Economou, Phys. Rev. A **20**, 2356 (1979).

²S. Liberman and J. Pinard, Phys. Rev. A **20**, 507 (1979).

³S. Feneuille, S. Liberman, J. Pinard, and A. Taleb, Phys. Rev. Lett. **42**, 1404 (1979).

⁴L. D. Landau and E. M. Lifshitz, *Kvantovaya mekhanika* (Quantum Mechanics), Nauka, Moscow, 1974 (Eng. Transl., Pergamon Press, Oxford, 1977).

⁵H. A. Bethe and E. E. Salpeter, *Quantum Mechanics of One- and Two-Electron Systems*, Springer Verlag, Berlin, 1958 (Russ. Transl., Fizmatgiz, Moscow, 1960).

⁶R. Ya. Damburg and V. V. Kosolov, *Asimptoticheskiĭ podkhod k zadache Shtarka dlya atoma vodoroda* (Asymptotic Approach to the Stark Problem for the Hydrogen Atom), Zinatne, Riga, 1977; *Teoreticheskoe issledovanie povedeniya vodorodnykh ridbergovskikh atomov v élektricheskikh polyakh* (Theoretical Investigation of the Behavior of Hydrogenous Rydberg Atoms in Electric Fields), Salaspils, 1980; J. Phys. B **9** 3149 (1976); **11**, 1921 (1978); **12** 2637 (1979); Opt. Commun. **24**, 211 (1978).

⁷E. Luc-Koenig and A. Bachelier, J. Phys. B **13**, 1743, 1769 (1980).

⁸M. H. Rice and R. H. Good, J. Opt. Soc. Am. **52**, 239 (1962).

⁹G. F. Drukarev, Zh. Eksp. Teor. Fiz. **75**, 473 (1978) [Sov. Phys. JETP **48**, 237 (1978)].

¹⁰D. A. Harmin, Phys. Rev. A **24**, 2491 (1981).

¹¹V. D. Kondratovich and V. N. Ostrovskii, Zh. Eksp. Teor. Fiz. **79**, 395 (1980) [Sov. Phys. JETP **52**, 198 (1980)].

¹²U. Fano, Phys. Rev. **124**, 1866 (1961).

¹³V. D. Kondratovich and V. N. Ostrovskii, VIII Vsesoyuzn. konf. po fizike élektronnykh i atomnykh stolknovenii. Tezisy dokladov (Abstracts of Papers Presented at the Eighth All-Union Conf. on Physics of Electronic and Atomic Collisions), Leningrad, 1981, p. 247; VII Vsesoyuzn. konf. po teorii atomov i atomnykh spektrov. Tezisy dokladov (Abstracts of Papers Presented at the Seventh All-Union Conf. on the Theory of Atoms and Atomic Spectra), Tbilisi, 1981, p. 61.

¹⁴I. Yu. Yurova, VI Vsesoyuzn. konf. po teorii atomov i atomnykh spektrov. Tezisy dokladov (Abstracts of Papers Presented at the Sixth All-Union Conf. on Theory of Atoms and Atomic Spectra), Voronezh, 1980, p. 88.

¹⁵M. B. Kadomtsev and B. M. Smirnov, Zh. Eksp. Teor. Fiz. **80**, 1715 (1981) [Sov. Phys. JETP **53**, 885 (1981)].

Translated by A. K. Agyei